JOURNAL OF MATERIALS SCIENCE 28 (1993) 3197–3204

Nondestructive evaluation of crazes and microcracks on polymers by the elastic-wave transfer function method

H.KAWABE, Y.NATSUME
NIPPONDENSO Co. Ltd, 1–1 Showa-cho, Kariya 448, Japan

Y.HIGO, S.NUNOMURA
Precision and Intelligence Laboratory, Tokyo Institute of Technology, 4259 Nagatsuta, Midori-ku, Yokohama 227, Japan

The precise study of the relation between microdefects such as crazes or microcracks and the elastic-wave transfer function method (ETFuM) was conducted in acrylonitrile butadiene styrene and acetal homopolymer. The ETFuM is the method of comparing the input elastic wave and the output wave from the specimens, and separating and analysing only the information on the object condition in the specimen from the transfer function in the frequency domain. In order to investigate the formation of crazes or microcracks caused by tensile deformation, transmission electron microscopy and polarization microscopy was used. The variation of transfer function before/after annealing indicated the dependence on the nucleation and growth of crazes or microcracks. The results suggested that ETFuM has potential as a useful method for the analysis of the micromechanism of the deformation process during nondestructive tensile and fatigue tests on polymers.

1. Introduction

Thermoplastic polymer is being used more and more frequently for applications where considerable loading is involved. However, the mechanical properties, especially the damaging fracture process, have not been clarified. For this reason the polymer has not been used for parts requiring reliability. When we consider the fracture process of a polymer, the formation of crazes or microcracks is thought to be a source of fracture. if we are able to evaluate microdefects such as crazes or microcracks quantitatively, we can elucidate the micromechanism of the deformation process during tensile and fatigue tests dynamically.

In this paper, crazes or microcracks due to tensile testing were monitored by the elastic-wave transfer function method (ETFuM) which compares the input elastic wave and the output wave from the specimens, and by then separating and analysing only the information concerned with the object condition in the specimen from the transfer function in the frequency domain. This method has the advantage of monitoring the specimen nondestructively, and furthermore, evaluating it under operating conditions without removing the structural components. In this study, polymers of acrylonitrile butadiene styrene (ABS) and acetal homopolymer (POM) were tested. The purpose of this study was to elucidate the relation between ETFuM and microdefects such as crazes or microcracks on the polymer.

2. Experimental procedure

2.1. Materials

Rods of commercially available ABS (ET-70, Mitsui Touatsu Chemicals Inc.) and POM (M-25, Polyplastics Co. Ltd) were used. Both materials are thermoplastic polymers. However, ABS is amorphous and POM is a crystalline polymer. The crystallinity of POM was found to be 63% by measuring the density at amorphous or crystalline domains. The mechanical properties of the materials used in this study are given in Table I. Specimens were machined from extruded 40 mm diameter rods of ABS and POM. Fig. 1 shows the dimensions of the test specimens used. The residual stress of the machined specimens was removed by annealing them under the conditions shown in Table II, and then cooling in the furnace.

2.2. The ETFuM

Fig. 2 shows schematically the transfer system of the elastic wave. In this figure, the respective functions in

TABLE I Mechanical properties of the polymers tested

	ABS	POM
Specific gravity	1.05	1.41
Tensile strength (MPa)	45.0	62.0
Modulus of elasticity (GPa)	2.0	2.8
Deflection temperature (°C)	93	158

0022–2461

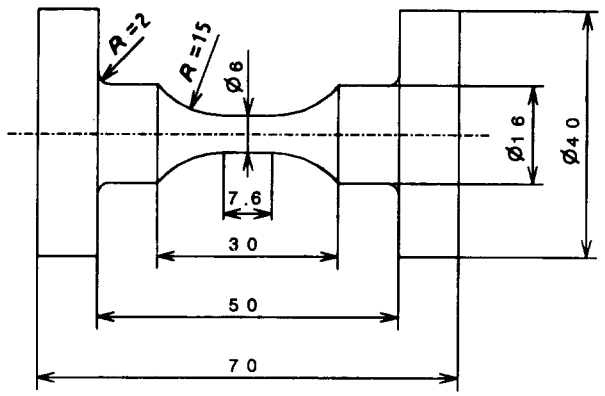

Figure 1 Shapes and dimensions of the test specimen.

TABLE II Annealing conditions

ABS	POM
80 °C, 3 h	140 °C, 3 h

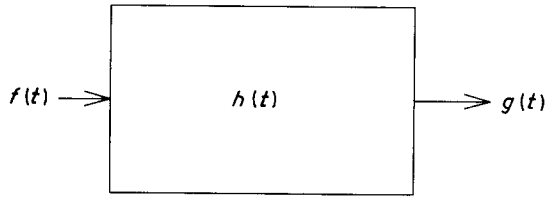

Figure 2 The relation between the input signal, $f(t)$, and output signal, $g(t)$. $h(t)$ is the transfer function of the object specimen.

time domain are

$$g(t) = \int_{-\infty}^{+\infty} h(t-\tau)f(t)\mathrm{d}\tau = h(t) \otimes f(t) \quad (1)$$

Then, they are transformed to frequency domains by performing a Fourier transform operation on the integral equation.

$$G(\omega) = H(\omega) \cdot F(\omega) \quad (2)$$

where, $G(\omega)$, $H(\omega)$ and $F(\omega)$ are the respective Fourier transforms of $g(t)$, $h(t)$ and $f(t)$. The input signal path is expected in Fig. 3 and is defined as

$$G_A(\omega) = M \cdot \beta_2 \cdot h_A \cdot \beta_1 \cdot S \cdot F(\omega) \quad (3)$$

where M and S are the received and transmitted transducer sensitivity, and β_1 and β_2 are transfer functions of the coupling condition between transducer and specimen. The transfer function of elastic signal through the specimen is expressed as

$$H_A(\omega) = G_A(\omega)/F(\omega) = S \cdot \beta_1 \cdot h_A \cdot \beta_2 \cdot M \quad (4)$$

The transfer function, H_A, is found by multiplying the transfer functions of the system components in the frequency domain as indicated in this equation. Information is only required concerning the polymer specimen h_A. Therefore, it is necessary to separate that

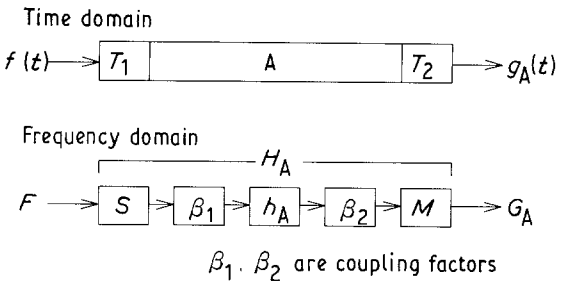

Figure 3 Schematic diagram showing elastic wave transmission through system A.

information from the characteristics of the transducers, and the coupling condition between the transducers and the specimen expressed as β_1 or β_2. We will use the same transducers shown here as S and M. In addition, we have developed a method of coupling the transducer to the specimen so as to obtain good acoustic reproducibility. The transfer function of H_{AN} including other specimens is defined in the same way as H_{A0} including a standard specimen. In this experiment, we used the transfer function on a virgin specimen as H_{A0}. Then all components of the transfer function that reflect the characteristics of the transducers S and M, and coupling conditions β_1 and β_2 are cancelled out, leaving only the information about the specimen as follows

$$\begin{aligned} H_{AN}/H_{A0} &= (G_{AN}/F_N)/(G_{A0}/F_0) \\ &= (S_N/S_0)\cdot(\beta_{1N}/\beta_{10})\cdot(h_{AN}/h_{A0}) \\ &\quad \cdot(\beta_{2N}/\beta_{20})\cdot(M_N/M_0) \\ &= (h_{AN}/h_{A0}) \end{aligned} \quad (5)$$

Also, the signal source, F, provides good reproducibility. The ratio of the output signal G_{AN} to G_{A0} directly explains the difference corresponding to the dynamic properties of the specimen.

$$G(\omega) = G_{AN}/G_{A0} = h_{AN}/h_{A0} \quad (6)$$

Therefore, the effects of specimen shape, transducer sensitivity and so on were eliminated in Equation 6. Then, the evaluation function H_{Af12} was defined as follows

$$H_{Af12} = \int_{f_2}^{f_1} |G(\omega)|\,\mathrm{d}\omega \quad (7)$$

where, H_{Af12} is an integrated value in a frequency range from f_1 to f_2 in Equation 6.

2.3. Method of measurement

The block diagram of the ETFuM measurement system is shown in Fig. 4. Two piezoelectric transducers were used as transmitter and receiver, respectively, and they were positioned in direct contact with the specimen using couplant grease. A signal, F, is generated by a function generator, input to the transmitting transducer, S, passes through the polymer specimen and is picked up by the receiving transducer, M, and amplifier. It is then fed into a FFT analyser along with the input signal. The signals are compared and only

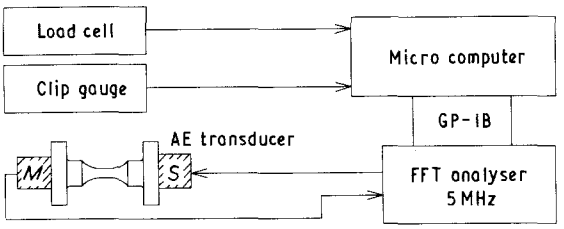

Figure 4 Block diagram of the ETFuM measuring system.

information on the specimen is extracted using Equation 5 or 6. The entire system is controlled automatically by a microcomputer.

Flat-type PZT transducers (0.01–5.0 MHz) were employed and the contact agent between the transducers and the specimen was W-400 (Nippon Steel Co. Ltd), which provided good reproducibility of the mounting conditions, for both the amplitude and phase components [1]. The measured data obtained with these transducers were sufficiently reliable for comparison without performing any special sensitivity calibration [2, 3]. In this study, f_1 and f_2 take values of 0.01 and 5.0 MHz in Equation 7, respectively.

The tensile tests were performed at 0.1 mm min^{-1} crosshead speed on the servo-hydraulic testing machine. Measurement of the transfer function was made for the pre-strained specimen, before and after annealing; the annealing conditions are given in Table II. All tests were performed at 20 °C.

2.4. Measurement of material properties

In order to elucidate the mechanical effects of annealing, two kinds of cyclic stress–strain curves were measured: in one test, annealing was conducted at every tensile test, whereas another test was conducted without annealing. Strain was applied until 6% in ABS, 10% in POM.

In order to determine the relationship between the transfer function and microdefects in ABS and POM, several experiments were performed. A Dunegan 8000 series AE testing system was used to measure the ultrasonic velocity. The ultrasonic velocity was determined from the time difference, by detecting the input signal with each side transducer. We also determined the elastic properties in a direction parallel to the ultrasonic transmitting direction. Elastic modulus, E, was calculated from the velocity from the equation

$$E = \rho V^2/k$$

$$k = (1 - \nu)/[(1 + \nu)(1 - 2\nu)] \quad (8)$$

where ρ is the density of the specimen, V the ultrasonic velocity, and ν is Poisson's ratio of the specimen [4]. Experimental data was used in Equation 8. The tensile test was performed at 0.1 mm min^{-1} crosshead speed on the servo-hydraulic testing machine. All tests were performed at 20 °C.

2.5. TEM observation and polarization microscopy

In order to investigate the relation between the transfer function variation and the formation of crazes or microcracks, microstructure was observed by TEM [5, 6]. Sections as thin as 1 μm were cut from a piece of the specimen secured on the microtome. The bulk structure specimen of ABS was cut in a parallel direction to the applied stress. The slices were exposed to osmium tetroxide vapour for at least overnight in order to stain them deeply.

For POM, a polarization microscope technique was used [7]. The same preparation procedure was followed as for ABS. Sections as thin as 10 μm were cut from a piece of the specimen secured on the microtome. The bulk structure specimen of POM was cut in a parallel direction to the applied stress.

3. Results

3.1. Tensile tests

Stress–strain curves of ABS and POM are shown in Fig. 5: stress increased gradually with increasing strain in both materials, as shown. Transition from elastic to plastic deformation was not clear, but it was relatively obvious in ABS. Plastic deformation started just before reaching maximum tensile stress in ABS. The fracture strain was 32% in ABS, and 33% in POM. The pre-strain level is shown as numbers 1–4 in the figure where (1) is the elastic region, (2) the region just before maximum tensile stress, (3) the maximum tensile stress, (4) after yield. After the applied stress was unloaded, the transfer function was measured.

3.2. Measurement of ETFuM

Fig. 6 shows an example of real-time measurement of the transfer function from the onset of the tensile test to unloading in both materials, as a plot of transfer function, G_A, in Equation 3 and stress against time from the tensile test onset. Stress was unloaded at maximum stress (strain level 3). The transfer function was measured from the onset of the tensile test to 600 min later. In ABS, the transfer function indicated 64.4 db at the initial state, and 57.7 db after unloading. On the other hand, the transfer function indicated 52.4 db at the initial state, and 49.4 db after unloading in POM. The change of the transfer function under tensile stress in POM was found to be less than in ABS. However, the transfer function decreased with increasing tensile stress in both materials. During unloading, the transfer function decreased, and then markedly recovered very quickly. Then, it became almost constant, no change even after 10 h. Thus the results indicate that the change in the transfer function after unloading was negligibly small. Therefore, measurement of the transfer function of pre-strained specimens was conducted within 1 h after unloading.

The relationship between the transfer function and pre-strain before or after annealing is shown in Fig. 7, as a plot of the function, H_{Af12}, in Equation 7 against pre-strain obtained from Fig. 5. In this experiment, the transfer function for a virgin specimen was taken as H_{A0} in Equation 5. The evaluation function decreased linearly with increasing pre-strain before annealing The trend was similar in POM, but the ratio of change was smaller than that in ABS. The virgin specimen

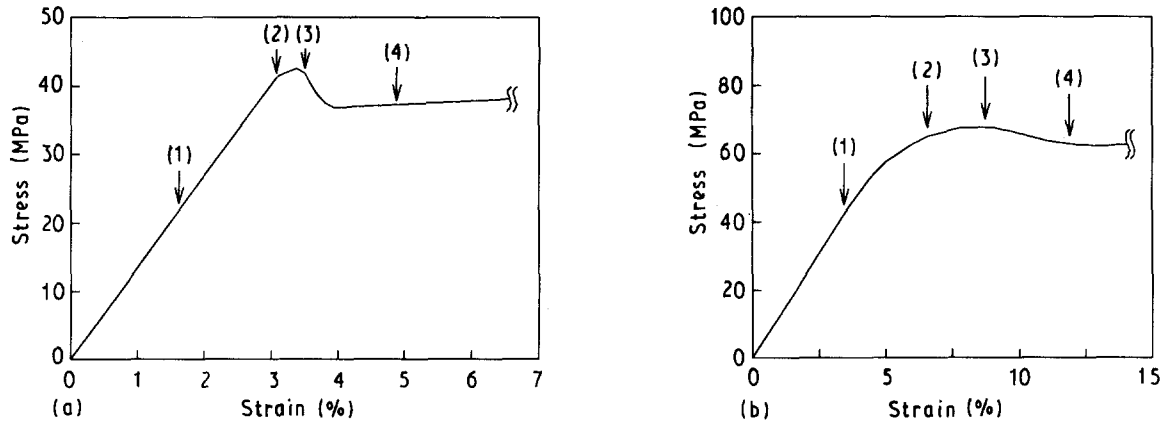

Figure 5 Stress–strain curves and pre-strained levels in (a) ABS and (b) POM. (1) Elastic region, (2) just before maximum tensile stress, (3) maximum tensile stress, (4) after yielding.

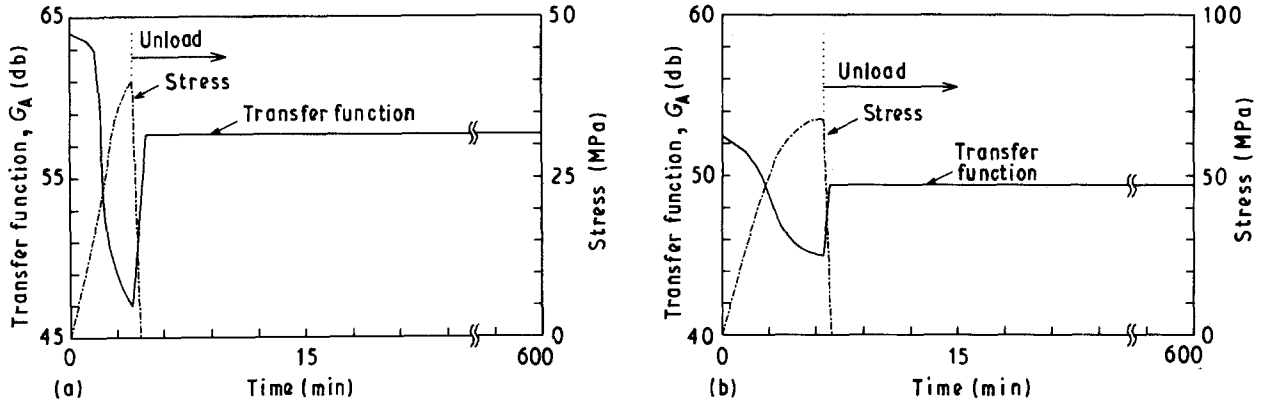

Figure 6 Example of real-time measurement of the transfer function from the start of the tensile test to unloading. Stress was unloaded from the maximum stress (strain level (3) in Fig. 5). (a) ABS, (b) POM.

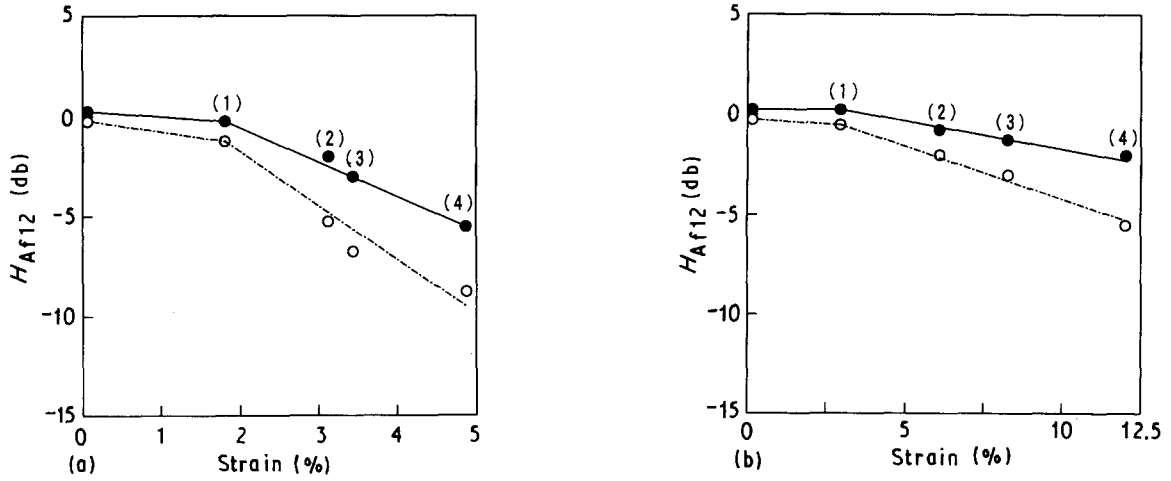

Figure 7 Relation between the transfer function and pre-strain, for (a) ABS, and (b) POM. (○) Before annealing, (●) after annealing. Numbers in the figure indicate the strain level shown in Fig. 5.

and elastically deformed specimen exhibited almost same value in both materials. On the other hand, the transfer function recovered after annealing in both materials, but did not regain the initial level on the pre-strained specimen.

3.3. Measurement of mechanical properties

In order to determine the effect of annealing on mechanical properties, tensile deformation and then the annealing process were repeated. Stress–strain curves of the virgin sample and then annealing in one specimen were measured; the curves are shown in Figs 8 and 9. Strain was applied until 6% in ABS, and 10% in POM in each tensile test. Annealing was carried out after each tensile test in Figs 8a and 9a. Figs 8b and 9b also show stress–strain curves without annealing. The number of tensile tests repeated on the same specimen is indicated in the figures. Significant differences in the stress–strain curves of the first and second tensile tests

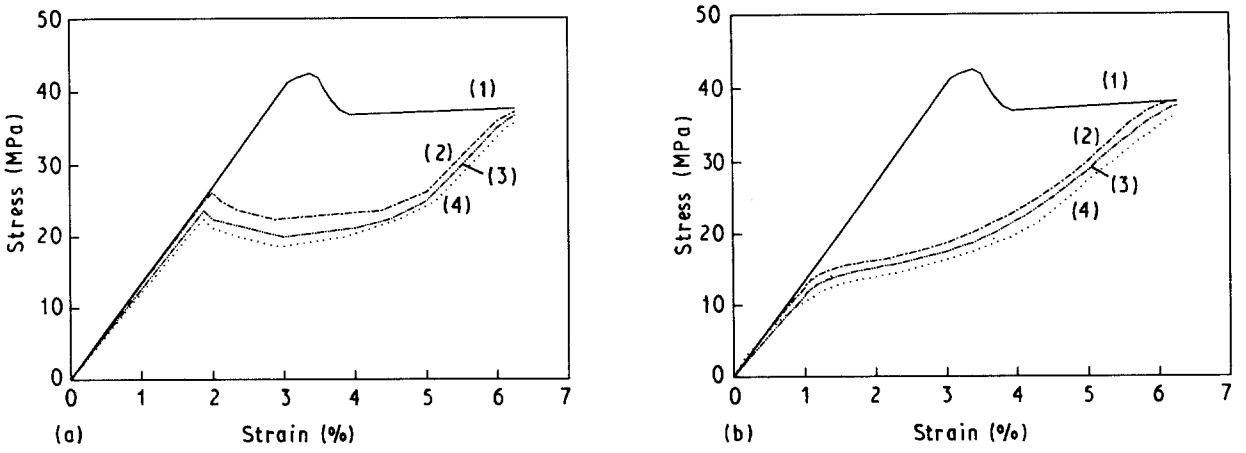

Figure 8 Cyclic stress–strain curves in ABS. Strain was applied until 6%. Numbers in the figure indicate the number of tensile tests repeated on the same specimen. (a) Annealing after each tensile test, (b) Without annealing.

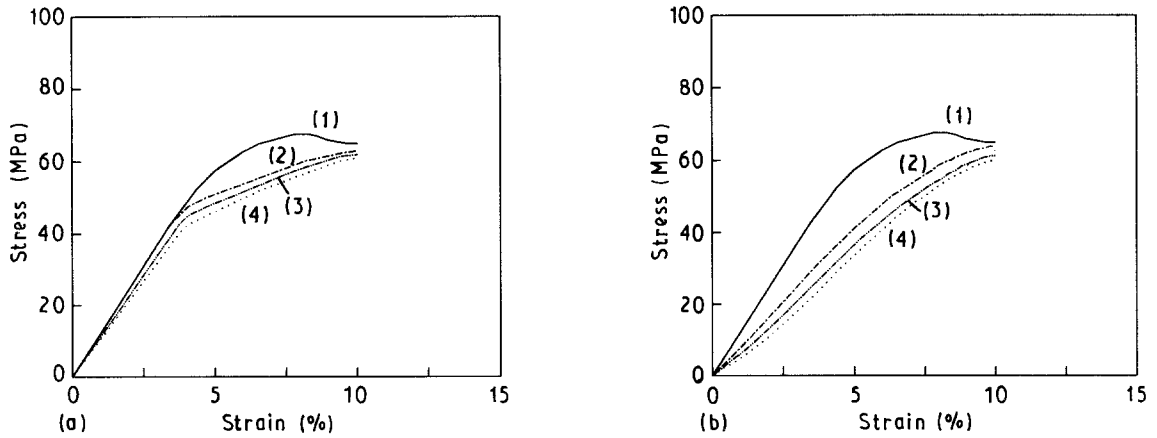

Figure 9 Cyclic stress–strain curves in POM. Strain was applied until 10%. Numbers in the figure indicate the number of tensile tests repeated on the same specimen. (a) Annealing after each tensile test, (b) Without annealing.

are seen. The effect of annealing on yield stress was not very large. However, in comparison, in the virgin specimen the yield stress increased to about twice its value before annealing. In Fig. 8a, yield stress (2–4) is 25–30 MPa. On the other hand, the yield stress is 10–15 MPa in Fig. 8b (2–4). After applying about 6% strain, the stress level reached was similar in all specimens (with and without annealing). In POM, annealing had an effect on the slope of elastic deformation region in the stress–strain curves. Without annealing, the elastic modulus decreased at each tensile test in Fig. 9b.

Fig. 10 shows the effects of annealing on ultrasonic velocity as a function of pre-strain. The velocity in ABS and POM decreases with increasing pre-strain. On annealing, the velocity in a 4.9% pre-strained specimen made approximately 80% recovery to the initial level in ABS. The more the pre-strain increased, the more the velocity made a recovery. However the initial level was not regained.

Fig. 11 shows the relation between elastic modulus and pre-strain. Elastic modulus was calculated using Equation 8 from the ultrasonic velocity shown in Fig. 10, and the measured density. In ABS and POM, results were similar to those for ultrasonic velocity. After annealing, the elastic modulus increased, but the initial level was not reached. On the other hand, elastic modulus in the virgin specimen obtained by tensile testing was 2.0 GPa in ABS, and 2.8 GPa in POM. It was reported that elastic modulus measured by tensile testing was very little different from that calculated using ultrasonic velocity in monotonic materials like metal. However, it did indicate a small difference in complex materials such as polymers or FRP [8].

4. Discussion

The micromechanism of the deformation process in polymers under tensile stress has been reported [9]. Molecular chains are slightly oriented in virgin specimens, and the oriented structure depends on the extrusion process. Therefore, the texture is thought to be almost homogeneous and isotropic in this study. With increasing strain, especially plastic strain, molecular chains will orient heterogeneously. It is considered that the oriented fibril structure, which is very similar to crazes, is constructed in a very fine area compared with crazes, and are thought to be embryos of crazing and to grow with increasing plastic strain, until they may be observed optically as crazes. As more stress was applied, the microcracks rapidly

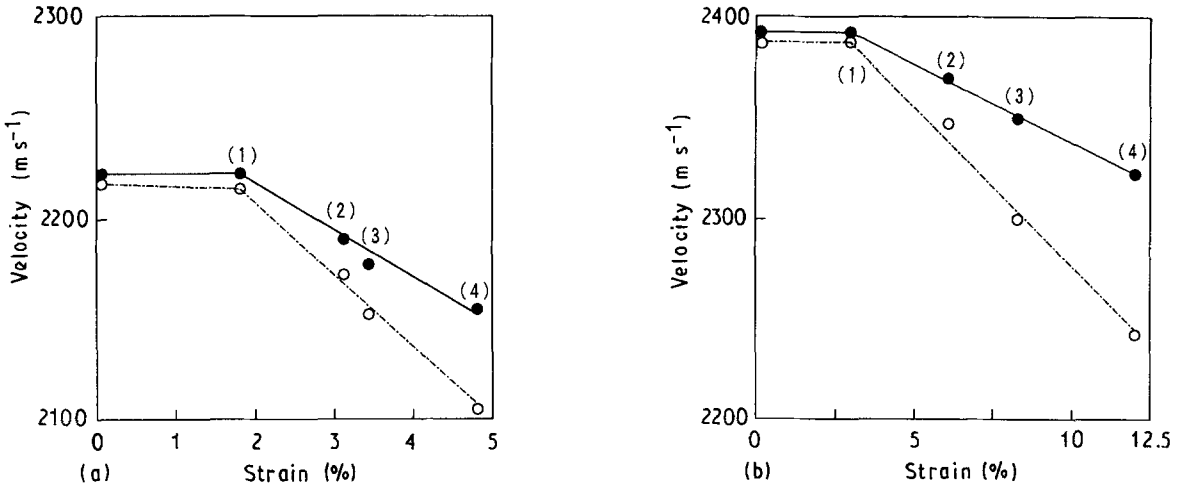

Figure 10 Relation between ultrasonic velocity and pre-strain, for (a) ABS, and (b) POM; (○) before annealing, (●) after annealing. Numbers in the figure indicate the strain level shown in Fig. 5.

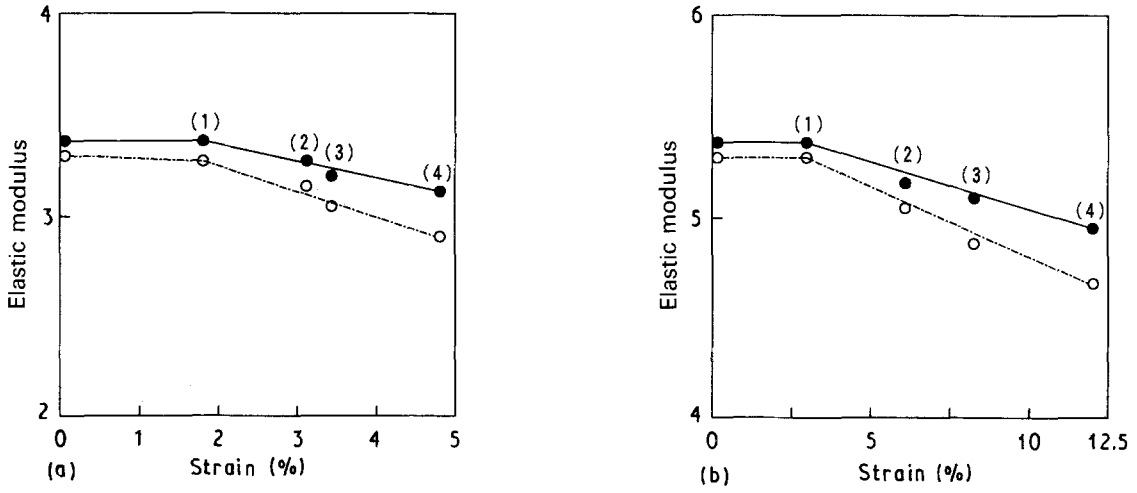

Figure 11 Relation between elastic modulus and pre-strain, for (a) ABS, and (b) POM; (○) before annealing, (●) after annealing. Numbers in the figure indicate the strain level shown in Fig. 5.

nucleated. We assume that the micromechanism of a large part of crazes has the reversible property on annealing; for example, most crazes disappear after annealing.

According to the transfer function measurement results shown in Fig. 7, the transfer function recovered after annealing in ABS and POM. In particular, in POM, the transfer function after annealing was very little different from the virgin specimen compared with ABS. This phenomenon is also observed in the tensile tests (Fig. 9). The stress–strain curves after annealing were quite similar to those of the virgin specimen. However, H_{Af12} and stress–strain curves in ABS did not recover after annealing (Figs 7a and 8). Therefore, the reversible property caused by annealing was recognized clearly as the transfer function.

To elucidate the relationship between changes in mechanical properties and the transfer function, several experiments were performed on specimens which had been used to measure the transfer function. The results suggested that part of the mechanical properties could recover on annealing. In order to determine the changes in mechanical properties in the direction parallel to the applied stress, we measured the changes of the ultrasonic velocity and elastic modulus (Figs 10 and 11). Both results were similar. After annealing, ultrasonic velocity and elastic modulus recovered, but did not recover to the initial level. These results suggested that the elastic modulus decreased because of a series connection of microcrack domains and amorphous or crystalline domains in the direction parallel to the applied stress, and that the elastic modulus is high at amorphous or crystalline domains, but is low at craze or microcrack domains after unloading. Because some microdefects were removed after annealing, the mechanical properties made a recovery. Therefore, some microdefects such as crazes have reversible properties, but some have irreversible properties.

In order to clarify the cause of the irreversible component, TEM was used for ABS. Fig. 12a shows an electron micrograph of a tensile specimen of ABS (4.9% pre-strained Fig. 5a, (4)). In Fig. 12a, crazes are seen to be nucleated on both sides of the rubber particles in a direction perpendicular to the applied stress. Because the elastic modulus of rubber is approximately 1/1000 of the resin phase, stress was concentrated in the matrix close to the interface

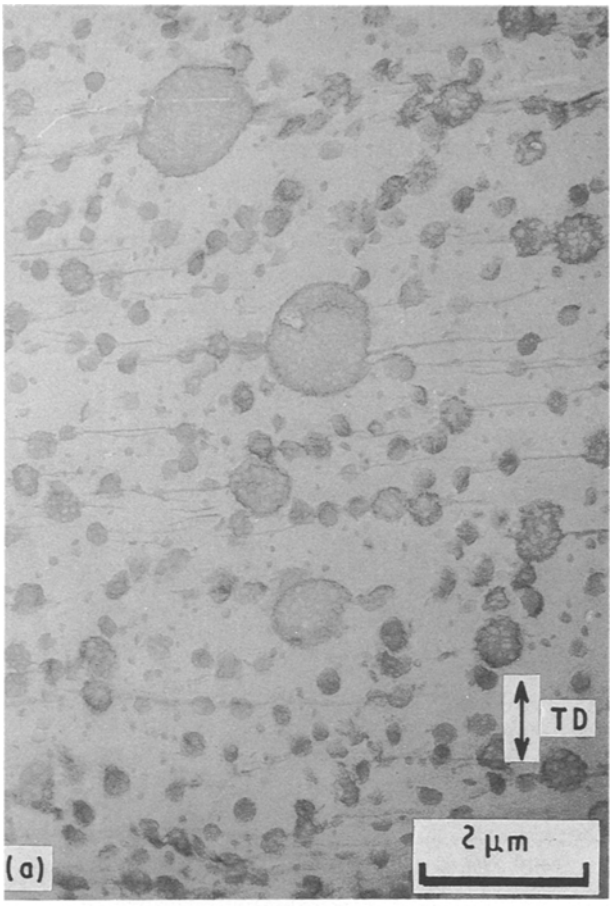

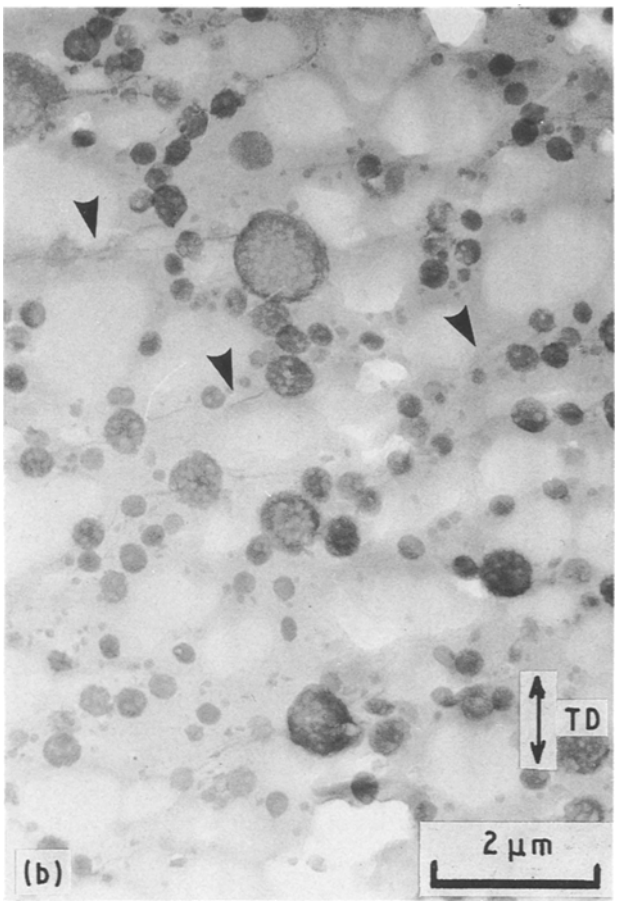

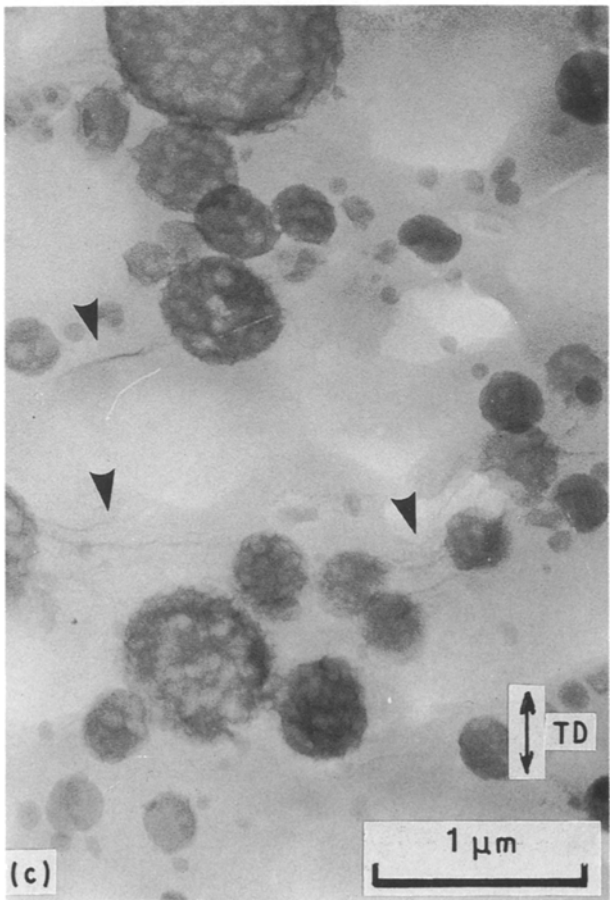

Figure 12 TEM observation in ABS. A 4.9% pre-strained specimen was observed. TD, tensile direction; arrows indicate microcracks. (a) Before annealing, (b) After annealing, (c) Higher magnification of (b).

between the rubber particles, and it presents a site for craze formation under tensile stress. Craze size was micrometre order. Fig. 12b shows an electron micrograph of the same specimen after annealing. Many crazes were removed by the annealing. As the rubber particles became hemispherical in shape, it was considered that strain was also removed. However, some microdefects remained in Fig. 12b and c (arrowed). They were considered to be not crazes but microcracks, because they remained after annealing. This phenomenon indicated the reason why the transfer function after annealing did not make a perfect recovery to the initial level. Thus, the electron micrograph agrees with the experimental results.

In POM, TEM observation was very difficult. Thus, the polarization microscope technique was used. Fig. 13 shows a polarization micrograph of a tensile specimen of POM (12.0% pre-strained Fig. 5b, (4)); the arrow indicates the tensile direction. Spherulitic texture was observed. This micrograph is similar to the results for the initial state, and fracture of the spherulite and orientation could not be observed clearly. Therefore, the texture did not indicate a significant change, as in ABS. The reason why a small variation of the transfer function indicated is due to the micromechanism of deformation.

Furthermore, the change in molecular structure was investigated by Fourier transform-infrared spectroscopy (FT–IR) [10], but changes were not confirmed in ABS or POM. Therefore, the change in the molecular structure did not occur by strain only, and any change did not affect the transfer function.

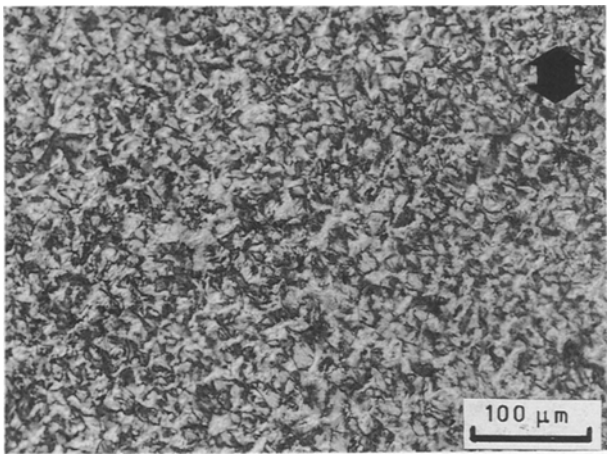

Figure 13 Polarization micrograph before annealing in POM. A 12.0% pre-strained specimen was observed. The tensile direction is indicated by the arrow.

All the results reported suggest that some microdefects in the polymer exhibited reversible properties on annealing, but some microcracks showed irreversible properties and the defects caused a decrease in the mechanical properties. ETFuM is therefore a useful method for nondestructive evaluation of reversible or irreversible properties of microdefects in polymers.

5. Conclusions

A new nondestructive evaluation method, elastic-wave transfer function method (ETFuM) has been applied to evaluate quantitatively crazes or microcracks in ABS and POM. The transfer function was very sensitive for monitoring the microdefects of pre-strained specimen in both ABS and POM. In particular, the transfer function indicated significant changes before and after annealing. The change is caused by the existence of crazes and microcracks in the materials which were confirmed by TEM. The elastic-wave transfer property depended on the reversible or irreversible properties of crazes and microcracks in the polymer. The results suggested that the ETFuM is a useful method for the nondestructive analysis of the micromechanism of a deformation process during tensile and fatigue tests on polymer. In particular, ETFuM evaluates irreversible damage such as microcracks in the polymer.

References

1. Y. HIGO and M. ONO, *Progr. AE Jpn Soc NDI* **3** (1986) 685.
2. Y. HIGO, S.KAZAMA and S. NUNOMURA, *Mater. Sci. Engng. A* **146** (1991) 327.
3. *Idem*, *Mater. Sci. Engng A* **146** (1991) 327.
4. "Ultrasonic Technology Manual" (The Nikkan Kogyo Shimbun Ltd, Tokyo, 1978).
5. K. KATO, *Polym. Engng Sci.* **7** (1967) 38.
6. M. MATSUO, *Polymer* **7** (1966) 421.
7. Y. HORI and M. KUBO, *Trans. Jpn Soc. Mech. Engng A* **474** (1986) 338.
8. S. HASEGAWA, N. NAKANO and A. KONDA, "Some Peculiarities of Sonic Modulus", Reports of Research Institute for Polymer and Textiles, Japan Foundation for Scientific and Technology Information, Vol. 8 (Tokyo, 1989) pp. 845–52.
9. H. KAWABE and Y. HIGO, *J. Mater. Sci.*, **27** (1992) 5547.
10. "Polymer Data Handbook" (The Society of Polymer Science Japan, Tokyo, 1986), pp. 643–53.

Received 26 February
and accepted 11 August 1992